

Investigation on wear and corrosion behavior of equal channel angular pressed aluminium 2014 alloy

S P Divya^{1,2,3}, G Yoganandan², J N Balaraju², S A Srinivasan¹, M Nagaraj¹, and B Ravisankar¹

¹Department of Metallurgical and Materials Engineering, National Institute of Technology, Tiruchirappalli, India

²Surface Engineering Division, National Aerospace Laboratories, Bangalore, India

³Corresponding author: perumaldivyagce@gmail.com

Abstract. Aluminium 2014 alloy solutionized at 495°C, aged at 195°C was subjected to Equal Channel Angular Pressing (ECAP). Dry sliding wear tests were conducted using pin on disc tribometer system under nominal loads of 10N and 30N with constant speed 2m/s for 2000m in order to investigate their wear behavior after ECAP. The Co-efficient of friction and loss in volume were decreased after ECAP. The dominant wear mechanism observed was adhesion, delamination in addition to these wear mechanisms, oxidation and transfer of Fe from the counter surface to the Al 2014 pin were observed at higher loading condition. The corrosion behavior was evaluated by potentiodynamic polarization (PDP) and electrochemical impedance spectroscopy (EIS) in 3.5% NaCl solution. The results obtained from PDP showed higher corrosion potential and lower corrosion density after ECAP than base. Electrochemical impedance spectroscopy (EIS) showed higher charge transfer resistance after ECAP. Surface morphology showed decreased pit size and increased oxygen content in ECAP sample than base after PDP.

1. Introduction

Equal Channel Angular Pressing is one of the emerging severe plastic deformation (SPD) techniques that improve mechanical and micro structural properties without changing the dimension of bulk unlike cold working, coating, surface treatments etc. For past decade EACP is efficiently employed for various alloys of aluminum to improve their properties by making it ultrafine grained material. Aluminum 2014 (Al-Cu alloy) is the material that is used for truck frames, aircraft structures, automotive parts, cylinders pistons, machine parts and structural applications due to its high strength imparted by CuAl₂ precipitates. ECAP improves hardness and tensile strength of Al 2014 alloy which has been reported [1]. Indeed, wear resistance is one of the important properties that influence the effective functioning of the material. Previous studies on the wear behavior of ECAPed materials reported that there is a significant improvement in wear resistance after ECAP, but some ended up with contradictory results i.e. ECAP can also decrease wear resistance in spite of its improved hardness due to lower ductility and lower strain hardening capability [2]. One the other hand, grain refinement plays vital role on the corrosion behavior of the material. Since ECAP tailors mechanical properties by the formation of ultrafine grains, equal importance must be given to their corrosion behavior, particularly in aluminum alloys where a protective oxide film imparts corrosion resistance. The effect of ECAP on the corrosion behavior of materials is still unclear. Corrosion current density has been shown to increase or decrease or remain unaffected in the presence of ultrafine grains. It has been reported that ECAP processing decreases the corrosion resistance of the base material due to high grain boundary area, internal stress, increased dislocation density and second phase that provide more sites to initiate corrosion [3]. However reports are also available to explain the improved corrosion resistance due to ECAP processing [4]. Nevertheless, study on the corrosion behavior of ECAPed aluminum copper alloys is scanty. Therefore, systematic study on the corrosion and wear behavior of aluminum alloys will be helpful to extend the knowledge on the frictional characteristics



and electrochemical behavior after ECAP. Hence, in the present investigation, an attempt has been made to study the wear and corrosion behavior of the ECAPed Al 2014 alloy and the results were compared with the base material.

2. Experimental procedure

Al 2014 alloy rod of diameter 15mm in stock condition and with following chemical composition (in wt%): Al-92.56%, Cu-4.7%, Mn-0.831%, Mg-0.751%, Fe-0.234%, Zn-0.0946% was taken for the present investigation. The as-received rods were machined to the diameter of 11.7mm and with the length of 70mm to match with die specifications. The samples were subjected to solutionizing at 495^o C, followed by ageing at 195^o C for 5 hours to attain peak hardness [1]. ECAP process was conducted in room temperature using a split die with an angle of 90^o between the two channels and 30^o outer arc of curvature. The sample and channels of die are coated with Molybdenum disulphide (MoS₂). Load of 30 tons was applied and samples were processed using route C for three passes. Route C follows 180^o rotations in same direction between every pass. The mechanical and micro structural properties were presented in our previous work [1]. Wear pins of 8mm diameter and 10mm height are made of ECAP samples for pin-on-disc wear test using DUCOM Vacuum tribometer with hardened EN 31 steel discs as counter body. The wear tests were conducted under the loads 10N and 30N for a sliding distance of 2000m at humidity of 65±5% and ambient temperature of 25±5°C. The circular samples for corrosion test were cut from the core of the ECAPed sample perpendicular to the direction of pressing and were polished using 1200 grit SiC emery sheets followed by ultrasonification in acetone for 10 minutes. Electrochemical tests such as potentiodynamic polarization and electrochemical impedance tests were carried out. Samples were immersed in all the solutions for 30 min before test to attain stable potential (open circuit potential). EIS studies were carried out in the frequency range of 100 kHz to 10 mHz. After EIS the system was allowed to reach steady state and then potentiodynamic polarization (PDP) tests were performed by scanning the electrode from -200mV to 200mV with respect to OCP. The sweep rate was 0.001V/s. The PDP plots obtained have been represented as potential vs current density and that of EIS as Nyquist plot (real vs. imaginary impedance). The surface morphology of the tested samples was analyzed by scanning electron microscopy (SEM) and energy dispersive X-ray analysis (EDAX) was used for elemental analysis.

3. Results and discussions

3.1. Wear behavior

3.1.1. Volume loss. Figure 1(a) shows vickers hardness of base and ECAPed sample. From the figure it is evident that the hardness of Al 2014 improved after 3 passes of ECAP from 95HVN to 165HVN. Figure 1(b) is the volume loss variation between base and ECAP after wear test under 10N and 30N. From the figure it can be understood that wear resistance improved after ECAP, as the volume loss decreased from 10.28±1 mm³ to 2.4±0.5 mm³ and 14.14±1 mm³ to 5.9±0.5mm³ under 10N and 30N loading conditions respectively. The volume loss increased with increase in load from 10N to 30N which is in good agreement with the Archard's law, $V=KLN/H$ where V= volume loss, K= wear coefficient, L=total sliding distance, N= applied load, H=hardness of the wear surface. It indicates that the volume loss depends on hardness and load applied. This decreased volume loss may be due to the combination of ageing and ECAP which produced higher hardness through grain refinement and precipitate fragmentation. It was reported that in Al 2014 alloy after ECAP the grain size decreased from ~10 μm to 0.23μm and the precipitate size reduced from 95±5nm to 45±5nm with uniform distribution its improved hardness [5].

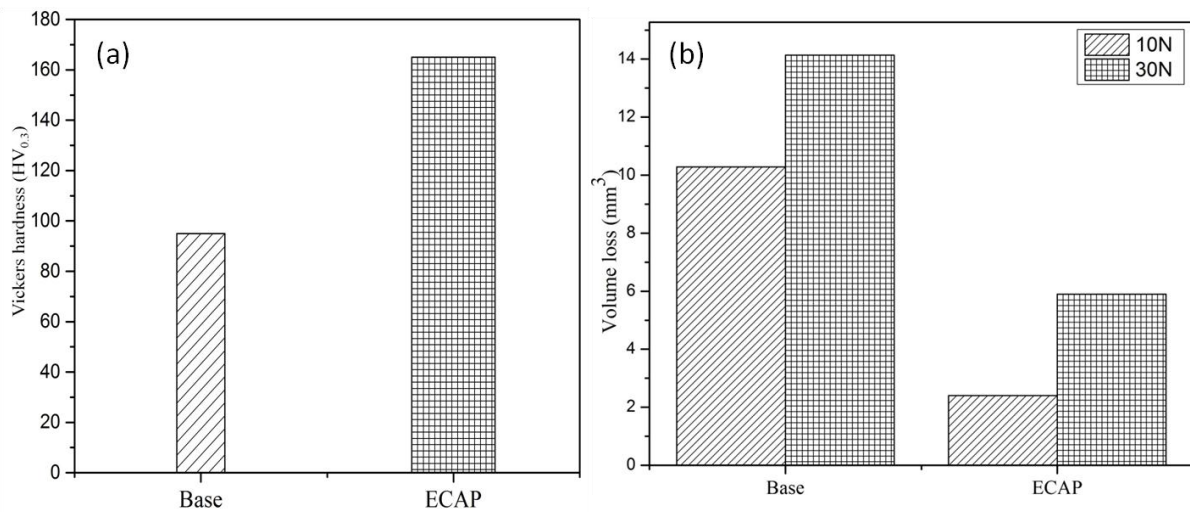


Figure1 (a) Hardness of Base and ECAPed sample (b) Volume loss of Base and ECAPed sample under 10N and 30N.

3.1.2. Coefficient of friction. Figure2 shows the variation in coefficient of friction (cof) of base and ECAPed sample. From the figure it can be observed that the coefficient of friction decreases after ECAP and it increases with increase in applied load. Under 10N the coefficient of friction vary between 0.35-0.45 for ECAP and 0.5-0.57 for base sample. The average value of cof decreases from 0.5 ± 0.03 (base) to 0.43 ± 0.04 (ECAP). In case of higher loading conditions the coefficient of friction of base varied between 0.5-0.65 upto sliding distance of 1000m which may resulted from adhesion, thus higher wear loss. However as the sliding distance increases, the cof decreases. This decrease in cof may be attributed to the formation of oxide layer on the surface[6]. But in ECAPed sample the cof varied between 0.45-0.5. The decrease in cof after ECAP may be attributed to strain hardening during sliding [6]. As the friction between the surface induce plastic deformation, higher grain boundary area and fine precipitates hinder dislocation. This leads to strain hardening of the material that are in contact which results in reduction of volume loss.

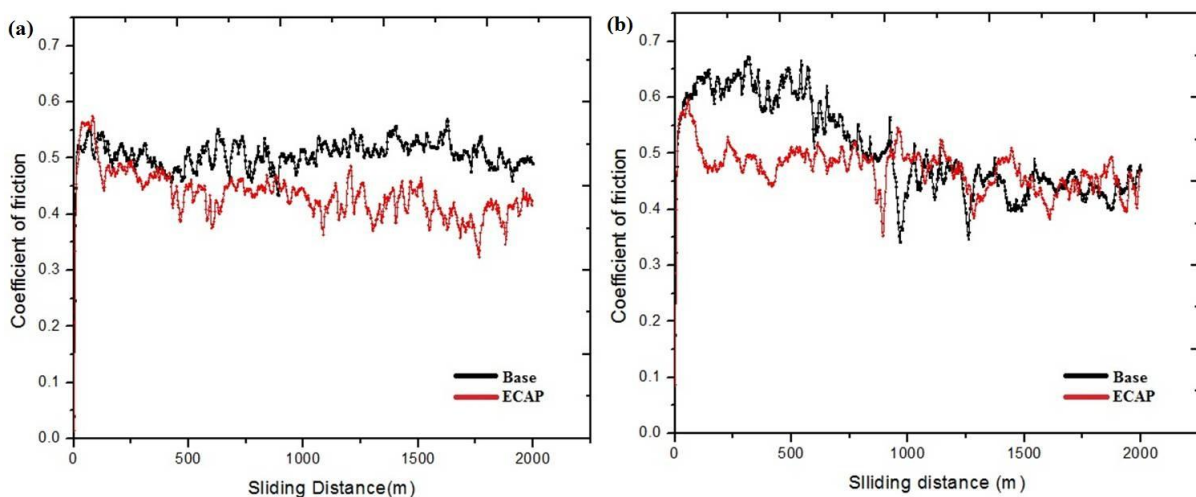


Figure2. Coefficient of friction of base and ECAP under (a) 10N (b) 30N.

3.1.3. Surface morphology. The figure3 shows the SEM images of wear tested surface of the base and ECAPed sample at applied load of 10N and 30N. The images demonstrate that the surface exhibit plastic deformation characterized by grooves formed by plowing in base under 10N and 30N. There

are evidences of craters that can be observed. During sliding at higher loads (30N), high tangential forces acting between the contacting surfaces results in nucleation of cracks at the subsurface. These cracks propagate parallel to the pin surface and cause delamination that result in detachment of debris and formation of craters [7]. This could be the possible reason for the higher cof up to 1000m under 30N. Comparing the processed sample with base, it appears that the severity of wear is less in ECAPed sample. There are few plastic deformations visible with smooth morphology of wear tracks, which confirms that the ECAP process improves wear resistance properties in Al 2014 alloy.

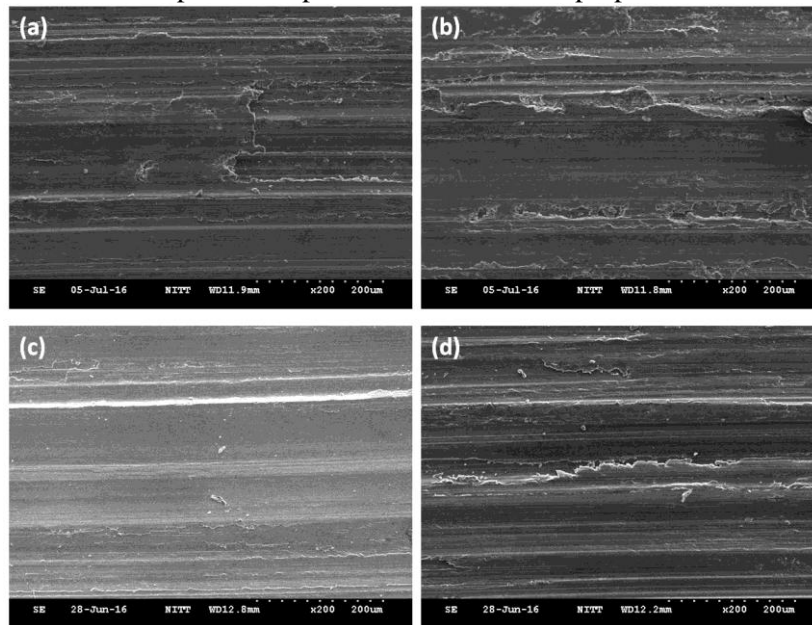


Figure3: SEM images of wear surface of (a)&(b) base under 10N and 30N (c)&(d) ECAPed under 10N and 30N.

3.1.4. EDS Analysis. The EDS spectra (Figure 4) showed presence of oxygen and iron on the surface which confirms that the mechanism include metal transfer and oxidation. The oxygen peak associates with the delamination and debris on the surface. The base sample showed higher oxygen content (24%) than ECAPed sample under 30N which may be resulted from the higher coefficient of friction in the initial stage. However the sample after ECAP posses less oxygen weight percentage of 15%.

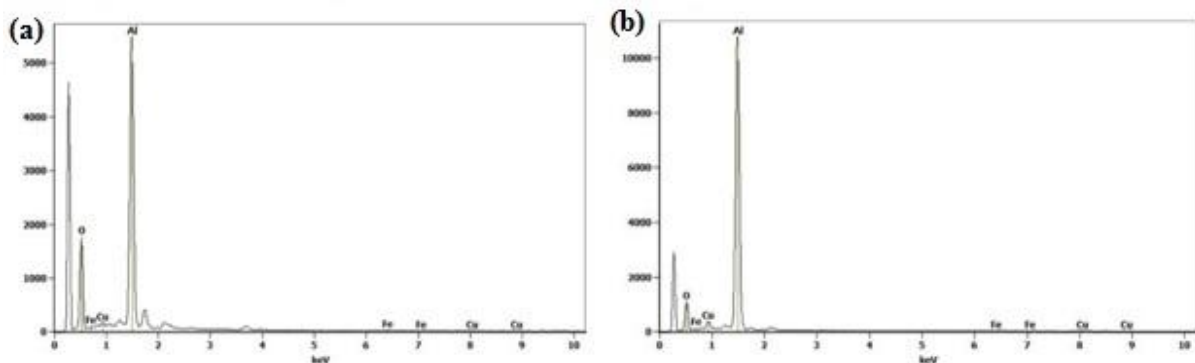


Figure 4: EDS analysis of surface after wear under 30N (a)base and (b) ECAP.

3.2. Corrosion behavior

3.2.1. EIS and PDP. Figure 5(a) show the Nyquist plot obtained from the EIS of base and ECAPed sample in 3.5% NaCl solution which is capacitive in nature. Sample processed by three passes of ECAP exhibit higher diameter arc which indicates its improved corrosion resistance after ECAP.

Impedance results showed two times constant behavior for both ECAP and base samples and the best fitted equivalent circuit $R[R(Q)][R(Q)]$ is shown in figure 5(a) insert. This behavior may be due to the formation of defective oxide layer during the immersion in electrolyte. The corrosion parameters obtained from EIS is tabulated in table 1(a). From the table it is evident that the R_{ct} and R_{ox} values obtained for ECAP sample is twice and four times higher than base sample respectively. In addition, Q_{dl} value reduced from 5900 to 2119 $\mu\text{S} \cdot \text{s}^n \cdot \text{cm}^{-2}$ after ECAP from which it is understood that the passive layer formed on ECAPed sample is stable and thick than that of base. Figure 5(b) shows PDP curves of base and ECAP and the obtained values are listed in table 1(b). From the figure it is evident that the cathodic curves shifts to lower current for the ECAPed sample resulted in decreased corrosion current density to $3.83 \mu\text{A}/\text{cm}^2$ which is half the i_{corr} value of base. This is in good agreement with the results obtained from EIS. It has been reported that the grain boundaries and high dislocation density after ECAP act as active sites for the formation of oxide layer which accelerates passivation and reduces corrosion rates [8]. It also reduces the intensity of galvanic couple formed between grain boundary and grain interior, precipitates and grains due to their ultrafine grain size and precipitate fragmentation along with uniform distribution. This may be the possible reason for the improved corrosion resistance after ECAP.

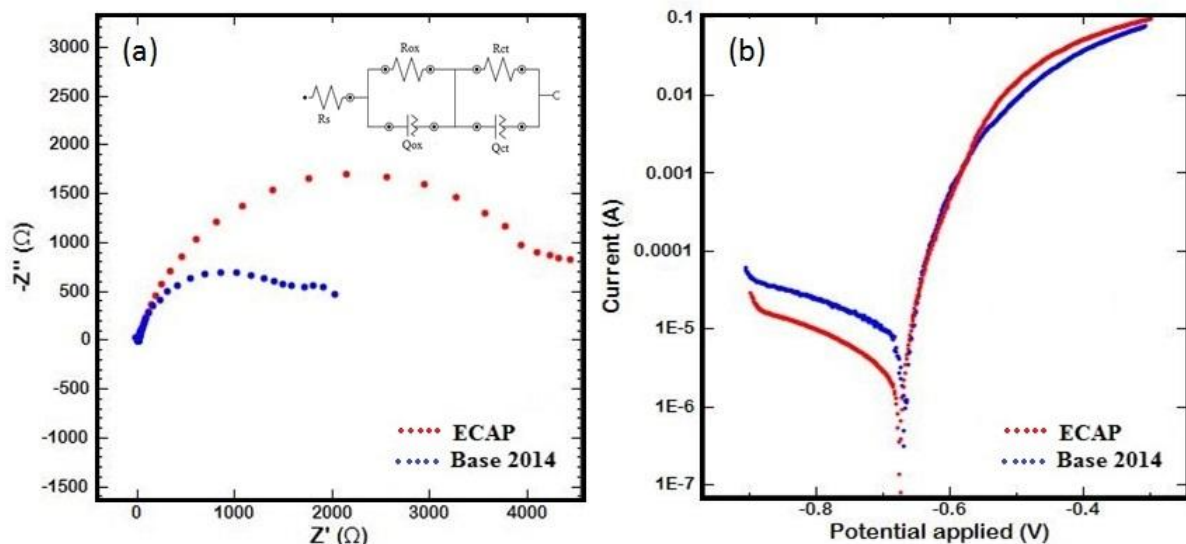


Figure 5: (a) PDP curve (b) Nyquist plot for Base and ECAP sample.

Table1: Corrosion parameters obtained from PDP and EIS.

Sample	(a) Parameters obtained from EIS							(b) Parameters obtained from PDP	
	R_s Ωcm^2	R_{ox} Ωcm^2	Q_{ox} $\mu\text{S} \cdot \text{s}^n \cdot \text{cm}^{-2}$	n_{ox}	R_{ct} Ωcm^2	Q_{dl} $\mu\text{S} \cdot \text{s}^n \cdot \text{cm}^{-2}$	n_{dl}	E_{corr} (V)	I_{corr} ($\mu\text{A}/\text{cm}^2$)
Base	3.3	1078	76	0.9	1000	5900	0.8	-0.67	8.6
ECAP	2.58	4162	30.89	0.85	2857	2119	0.72	-0.67	3.83

3.2.2. Surface morphology and EDS Analysis. Figure6 shows the SEM images of the surface obtained after PDP. The surface morphology of both base and ECAPed sample showed cracks and pits. But the pits observed in ECAPed sample was significantly small than that observed in base. The average size

of the pits on the base was found to be $20\pm 4\mu\text{m}$ and that of ECAPed sample was $3\pm 2\mu\text{m}$. The formation of pits may be due the galvanic couple formed between the cathodic precipitates and anodic matrix [9] which is evident from the EDS analysis as shown in figure 7. It shows 18% of copper and 49% of aluminum and 24% of oxygen in the spot analysis of pits. Also the EDS analysis on the surface of ECAP sample showed higher oxygen content of 24% than the base sample (8.26%). Hence it can be concluded that the improved corrosion resistance after ECAP is due to the oxide layer formed on the surface due to ultrafine grains which are consistent with the results obtained from EIS.

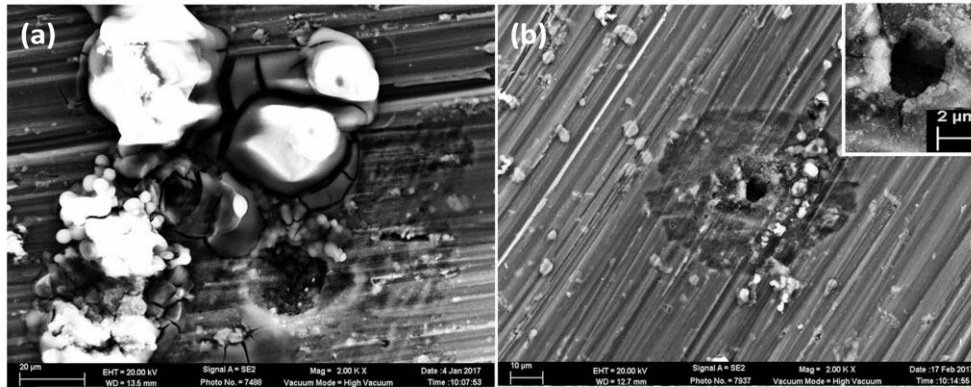


Figure6: SEM image of (a) base and (b) ECAP samples after potentiodynamic polarization test.

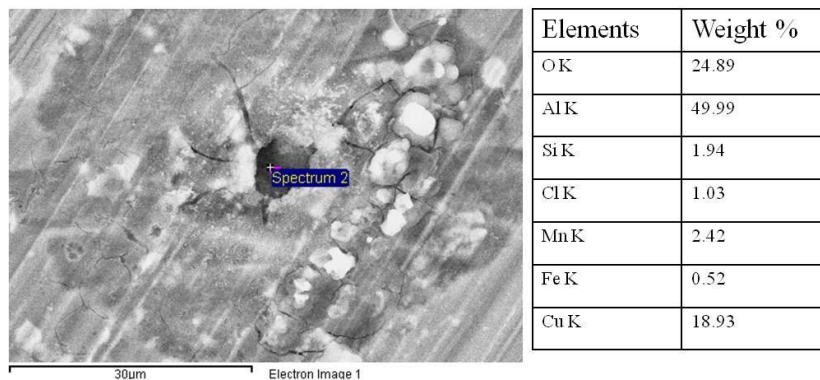


Figure 7: EDS analysis of pit on the ECAPed sample after PDP.

4. Conclusion

1. The pin on disc sliding wear test showed decreased volume loss and coefficient of friction after ECAP under both the loading conditions 10N and 30N due to improved hardness during ECAP. The SEM analysis of the worn surface revealed smooth morphology of wear tracks after ECAP and EDS analysis confirmed oxidation and metal transfer.
2. PDP results showed higher E_{corr} and lower i_{corr} values after ECAP. EIS results showed higher charge transfer resistance (R_{ct}) for ECAPed sample. SEM analysis revealed significantly smaller pits in ECAPed sample than that of base.
3. Higher oxygen content was observed after corrosion test in ECAPed sample than base sample in EDS analysis.
4. Hence it can be concluded from the above results that Al 2014 alloy showed improved wear and corrosion resistance after ECAP.

References

- [1] Venkatachalam P, Ramesh Kumar S, Ravisankar B, Thomas Paul V and Vijayalakshmi M 2010 Effect of Processing Routes on Microstructure and Mechanical Properties of 2014 Al Alloy Processed by Equal Channel Angular Pressing, *Trans. Of Nonferrous Met. Scc China* **20** 1822-28.
- [2] Gao N, Wang C T, Wood R J K and Langdon T G 2012 Tribological Properties of Ultrafine-grained Materials Processed by Severe Plastic Deformation, *J. Mater. Sci.* **47** 4779–97.
- [3] Atef Korchef and Abdelkrim Kahoul 2013 Corrosion Behavior of Commercial Aluminum Alloy Processed by Equal Channel Angular Pressing, *International Journal Of Corrosion* Article Id 983261**2013** 1-11.
- [4] Min-Kyong Chunga, Yoon-Seok Choi A, Jung-Gu Kima,, Young-Man Kimb and Jae-Chul Lee 2004 Effect of the Number of ECAP Pass Time on the Electrochemical Properties of 1050 Al Alloys *Materials Science And Engineering A* **366** 282–291.
- [5] Venkatachalam P, Shibayan Roy, Ravisankar B, Thamos Paul V, Vijayalakshmi M and Suwas S 2012 Effect of Processing Routes on Evolution of Texture Heterogeneity in 2014 Aluminium Alloy Deformed by Equal Channel Angular Pressing (ECAP) *Materials Science and Technology* **28** 1446-58.
- [6] Van Thuong N, Zuhailawati H, Seman A A, Huy T D and Dhindaw B K 2015 Microstructural Evolution and Wear Characteristics of Equal Channel Angular Pressing Processed semi-solid-cast Hypoeutectic Aluminum Alloys *Mater. Des.* **67** 448–456.
- [7] Nam. P. Suh 1977 An Overview of the Delamination Theory of Wear, *Journal wear* **44** 1-16.
- [8] Palumbo G, Thorpe S J and Aust K T 1990 On the Contribution of Triple Junctions to the Structure and Properties of Nanocrystalline Materials *Scripta Metallurgica et Materialia* **24** 1347-50.
- [9] Jiang Jing-Hua, Ma Ai-Bin, Song Dan, N. Saito, Yuan Yu-Chun and Nishida Y 2010 Corrosion Behavior of Hypereutectic Al-23%Si Alloy (AC9A) Processed by Severe Plastic Deformation *Trans. of Nonferrous Metals Society of China* **20** 195-200.